Transactions of the Korean Nuclear Society Spring Meeting
Chuncheon, Korea, May 25-26 2006

Monte Carlo Investigation of Phosphor Screens for X-ray Imaging

Chang Hwy Lim, Min Ho Cheong, Min Kook Cho, Choel-Soon Shon, Ho Kyung Kim*
School of Mechanical Engineering, Pusan National University
**Corresponding Author: hokyung@pusan.edu*

1. Introduction

In order to detect X rays with pixel detectors, there are two technical methods; a direct detection using photoconductive material that permits the conversion of the incident X rays into the signal charges, and an indirect detection using scintillation material that converts the incident X rays into the optical photons. Therefore, two-dimensional (2D) photosensitive pixel array is necessary for the indirect-detection scheme. Terbium-doped gadolinium oxysulfide (Gd_2O_2S:Tb) phosphor screen is the most popular X-ray converter, and often employed to the digital radiographic system owing to its well-known technology and easy handling in size, thickness, and flexibility [1]. Furthermore, the cost is effective.

In cascaded imaging chains of the indirect-detection system, the phosphor screen is served as the first stage. Since the image signal-to-noise ratio (SNR) is irreversible through the cascaded system, the phosphor screen is largely responsible for the eventual image quality. For the various radiation qualities suggested by IEC (International Electrotechnical Commission, Report 1267) [2], we have investigated important physical quantities of Gd_2O_2S:Tb screen with a wide range of coverages (34 – 135 mg/cm^2) by using Monte Carlo calculations. The results will be useful for the optimal design of digital X-ray imaging systems.

2. Methods

We have investigated the performance of Gd_2O_2S:Tb screens in terms of quantum absorption A_Q and energy absorption A_E, Swank factor A_S, and DQE (detective quantum efficiency) [2]. These performances can be evaluated by using energy moments of the absorbed energy distribution (AED) $S(E)$, which is the distribution of deposited energy from the incident X-ray quanta through interaction mechanismas such as photoelectic absorption and Compton scattering. It is noted that the pair production can be neglected in the diagonostic radiology. Because of high rate of X rays, expensive experimental setups, and tremendous efforts on the analysis, the AED is, however, difficult to be directly measured. Instead, it is normally estimated by Monte Carlo simulations. With $S(E)$, the performances of the phosphor screen can be calculated as follows [2]:

$$A_Q = M_0 \quad (1)$$

$$A_E = M_1 / M_0 \quad (2)$$

$$A_S = M_1^2 / (M_0 M_2) \quad (3)$$

$$\mathrm{DQE} = A_Q A_S = M_1^2 / M_2 \quad (4)$$

where $$M_n = \int_E E^n S(E) dE \quad (5)$$

In order to determine the AED of the phosphor screen with a wide range of coverages (see Table 1), we used MCNPX^{TM} (Version 2.4.0, ORNL, USA), which simulates X-ray interactions in the phosphor screen. We considered a pencil beam incident perpendicularly onto the phosphor screen and we modeled the screen as a thin slab with infinite lateral dimension. As summarized in Table 1, the phosphor screens have very small thicknesses, a 20-cm radius is enough. For the realistic source sampling covering the overall energy range in diagnostic radiology, we accounted for all the RQA series of X-ray spectra suggested by IEC. Approximate tube voltage of the series ranges from 40 to 150 kV. The detailed parameters are shown in Table 2. The normalized X-ray spectra were generated by the self-developed computational program for X-ray spectral analysis (*Xtailor*, BML, PNU) [3]. The resulting AED of the phosphor screen was used to estimate the energy moments and performance quantities discussed above by simple numerical integration and division.

Table 1. Summary of phosphor screen types and physical parameters.

Scintillation screen types	Physical parameters		
	Coverage [mg/cm^2]	Thickness [μm]	Density [g/cm^3]
Min-R^{TM} 2000	33.9	84	4.04
Min-R^{TM}	33.9	90	3.77
Lanex^{TM} Medium	59.2	160	3.70
Lanex^{TM} Regular	70	180	3.89
Lanex^{TM} Fast Back	134.6	300	4.48

Table 2. Characterization and parameters for standard radiation qualities suggested by IEC.

Standard radiation quality	Half-value layer (mmAl)	Added filter (mmAl)	Approximate tube voltage (kV)
RQA 2	2.4	4	40
RQA 3	4.0	10	50
RQA 4	5.7	16	60
RQA 5	7.1	21	70
RQA 6	8.4	26	80
RQA 7	9.1	30	90
RQA 8	9.9	34	100
RQA 9	11.5	40	120
RQA 10	12.8	45	150

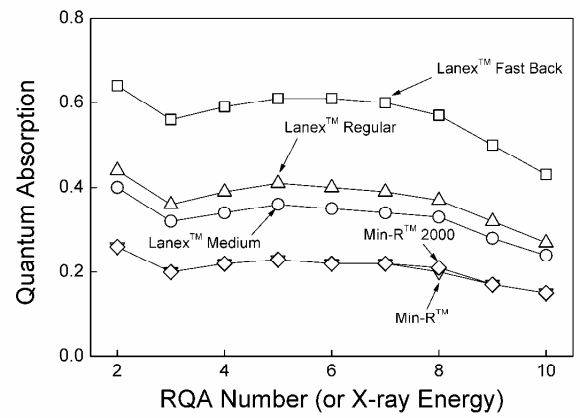

Fig. 1. Quantum absorption as a function of energy.

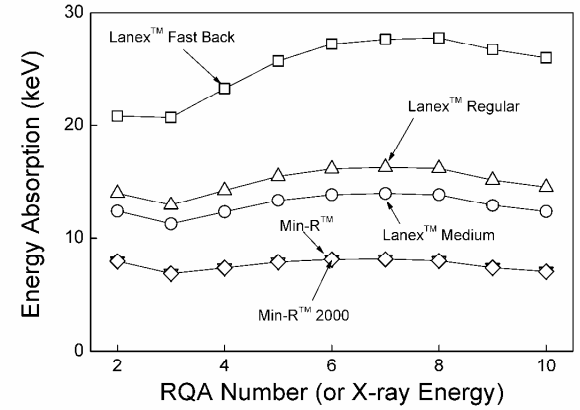

Fig. 2. Energy absorption as a function of energy.

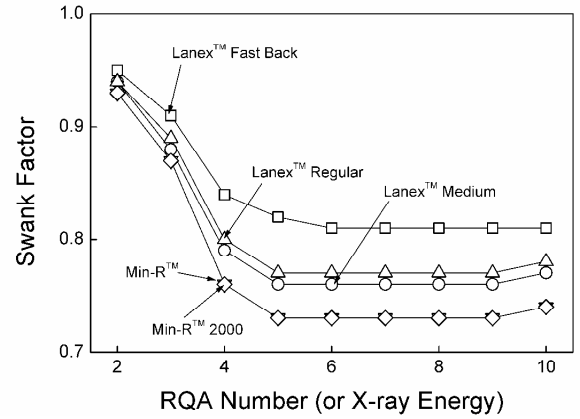

Fig. 3. Swank factor or statistical noise as a function of energy.

3. Results and Discussion

Figure 1 shows the quantum absorption as a function of energy (or RQA series). The general trend is independent of the phosphor thickness. Investigation of the AED revealed that gradual increase of the quantum absorption from RQA 2 to RQA 5 is due to the reabsorption of *K*-edge fluorescence of gadolinium. The decrease after RQA 5 is presumed to lower interaction probability of the higher X-ray quanta. These trends are similarly applied to the energy absorption as shown in Fig. 2. From the Eq. (3), Swank noise is strongly related to the variance of AED. At lower energy region, it is rapidly decreased as the energy increases, and after RQA 5, it becomes independent on the energy. See Fig. 3. These phenomena are well understood by investing the AEDs. The details will be presented at the conference. DQE describing SNR^2 of X-ray energy absorption obeying the Poisson statistics for the incident X-ray quanta is shown in Fig. 4, which shows that the DQE is almost determined by the phosphor thickness.

4. Conclusion

Using Monte Carlo calculations, we have investigated the performance of Gd_2O_2S:Tb screens with a wide range of thicknesses in terms of quantum absorption, energy absorption, Swank noise, and DQE. Calculations showed that the performances were proportional to the increase of the thickness. The results will be useful for the optimal design of digital X-ray imaging systems. However, since those quantities are related to the sensitivity and SNR, the resolution property should be separately investigated for the given imaging tasks.

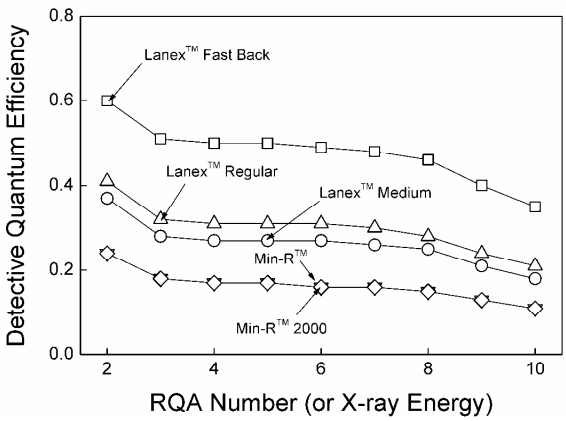

Fig. 4. Detective quantum efficiency as a function of energy.

ACKNOWLEDGMENT

This work has been supported by KESRI (Grant No. R-2005-7-022), which is funded by MOICE.

REFERENCES

[1] H. K. Kim, J. K. Ahn, and G. Cho, "Development of a lens-coupled CMOS detector for an x-ray inspection system," Nucl. Instr. Meth. A 545, pp. 210-216 (2005).

[2] G. Cho, H. K. Kim, Y. H. Chung, D. K. Kim, H. K. Lee, T. S. Suh, and K. S. Joo, "Monte Carlo analyses of x-ray absorption, noise, and detective quantum efficiency considering therapeutic x-ray spectrum in portal imaging detector," IEEE Trans. Nucl. Sci. 48, pp. 1423-1427 (2001).

[3] C. -S. Shon, H. K. Kim, M. K. Cho, M. H. Cheong, and J. -M. Kim, "Design of a computational toolset for x-ray spectral analysis," The First International Conference on Advanced Nondestructive Evaluation, Jeju, Korea, November 7-9, 2005.